Journal of the Australian Ceramic Society (2022) 58:597–605
https://doi.org/10.1007/s41779-022-00719-0

RESEARCH

Crystallization behaviors and properties of Ti-bearing blast furnace slag-based glass ceramics with varying CaO/SiO_2 mass ratio

Xin Feng[1,2] · Feifei Lai[1,2] · Jiangling Li[1,2] · Qingcai Liu[1,2] · Shan Ren[1,2] · Jian Yang[1,2]

Received: 24 August 2021 / Revised: 21 January 2022 / Accepted: 13 February 2022 / Published online: 23 February 2022

Abstract

The effect of CaO/SiO_2 ratio on the crystallization behaviors, mechanical properties, and acid and alkali resistance properties of the prepared Ti-bearing blast furnace slag-based glass ceramics were investigated. The results showed that the crystallization temperature obviously decreased with the increase of CaO/SiO_2 ratio, and the higher CaO/SiO_2 ratios leaded to stronger crystallization ability. The main crystal phases transformed from $CaAl_2Si_2O_8$ and $CaMgSi_2O_6$ to $CaAl_2Si_2O_8$, $CaMgSi_2O_6$, and $Ca_2MgSi_2O_7$ as the CaO/SiO_2 ratio increased from 0.3 to 0.6. When the CaO/SiO_2 increased to 0.5, a small amount of akermanite precipitated. The vickers hardness gradually decreased, and the flexural strength first increased and then decreased with an increased CaO/SiO_2. The glass ceramic with $CaO/SiO_2 = 0.5$ exhibited the highest flexural strength of 109.58 MPa. The prepared glass ceramics showed good acid and alkali resistance (> 98.30%), especially alkali resistance. Therefore, the best candidate for CaO/SiO_2 ratio in the investigated Ti-bearing blast furnace slag-based glass ceramics was selected as 0.5. This work can provide the reference for preparation slag-based glass ceramics.

Keywords Glass ceramics · Ti-bearing blast furnace slag · CaO/SiO_2 · Crystallization

Introduction

Glass ceramic is a composite material composed of a mini-crystal phase and residual glass phase, which is made by controlling the crystallization of basic glass with a specific composition during the heating process [1–5]. Because its performance combines the advantages of glass, ceramic, and stone, it can be used as a building material, a functional material, and a structural material.

A large amount of metallurgical solid waste is accumulated and cannot be efficient utilization in ironmaking industry, which resulted in environment pollutions and resource waste [6–9]. Ti-bearing blast furnace slag is one of the metallurgical solid wastes produced in the blast furnace ironmaking process using vanadium-titanium-bearing magnetite. The main components of Ti-bearing blast furnace slag are SiO_2, CaO, MgO, and Al_2O_3, which are also important components of silicate-based glass ceramics [10–12]. In addition, a small amount of TiO_2 can be a good crystal-nucleating agent, which can promote nucleation and crystallization [13, 14]. In this work, the low Ti-bearing blast furnace slag was applied to prepare glass ceramics, which includes approximately 6% TiO_2. This kind of low content TiO_2 can be used as nucleating agent for the preparation of glass ceramics, and no additional nucleating agent is required. In addition, compared to steel slag, low Ti-bearing blast furnace slag has a lower alkalinity, which is closer to the alkalinity of silicate-based glass ceramics. Therefore, the low Ti-bearing blast furnace slag has great potentials to prepare slag-based glass ceramic.

The performance of glass ceramics largely depends on crystallization behaviors of basic glass [6, 15]. The crystallization behaviors of glass are mainly affected by nucleation and crystal growth, and the main influencing factors include nucleation agents, components, and heat treatment process [16–19]. According to previous reports, SiO_2 was the main oxide in silicate glass, and its structure in glass had a decisive influence on the properties of silicate glass [20–22]. CaO existed in silicate network as a network modifier, which can polarize bridging oxygen and weaken Si–O bond [23,

✉ Jiangling Li
lijiangling@cqu.edu.cn

1 College of Materials Science and Engineering, Chongqing University, Chongqing 400044, People's Republic of China

2 Chongqing Key Laboratory of Vanadium-Titanium Metallurgical and New Materials, Chongqing University, Chongqing 400044, People's Republic of China

24]. SiO_2 and CaO were as the main components of silicate-based glass ceramics, and played important roles in the crystallization process of glass ceramics [24–27]. Li et al. [28] reported that the microstructure, mechanical, thermal, and electrical properties of $BaO\text{-}Al_2O_3\text{-}B_2O_3\text{-}SiO_2$ glass ceramics were improved, and the flexural strength and the Young's modulus of glass ceramics remarkably increased from 67 to 150 MPa and 45 to 66 GPa, respectively, with the increasing SiO_2 content. Zhou et al. [29] investigated the effect of CaO/SiO_2 ratio on the microstructures, electrical properties, and mechanical characteristics of the $CaO\text{-}B_2O_3\text{-}SiO_2$ glass ceramics which synthesized by sol–gel method, and indicated that the increase of CaO content promoted the crystallization and increased the flexural strength. Hou et al. [30] studied the effect of different CaO/SiO_2 ratio and heat treatment parameters on the main crystalline phase of $SiO_2\text{-}CaO\text{-}Al_2O_3\text{-}Na_2O$ glass ceramics, and showed that the existence of nepheline had enhanced the mechanical properties of glass ceramics. Fu et al. [31] optimized CaO/SiO_2 ratio and B_2O_3 content of $CaO\text{-}B_2O_3\text{-}SiO_2$ glass ceramics, and reported that the crystallization ability of glasses increased with the increase of B_2O_3 and CaO/SiO_2 ratio, which resulted in an increased permittivity of glass ceramics. Besides, the influence of CaO/SiO_2 ratio on the preparation of glass ceramics from traditional blast furnace slag has been investigated, including crystallization ability, crystal phase, and mechanical properties [10, 32, 33]. However, the effect of CaO/SiO_2 ratio on the properties of Ti-bearing blast furnace slag-based glass ceramics has been less reported.

In our previous work [34], the influence of TiO_2 on the crystallization behavior of Ti-bearing blast furnace slag-based glass ceramics had been investigated and showed that the good performance and crystallization behaviors of glass–ceramic were obtained when the content of TiO_2 was about 4%. To further explore the influence of CaO/SiO_2 mass ratio on the Ti-bearing blast furnace slag-based glass ceramics, a series of Ti-bearing blast furnace slag-based glass ceramics with varying CaO/SiO_2 mass ratio were prepared. Additionally, the variation range of CaO/SiO_2 ratio were also considered by that the content of TiO_2 can be maintained at approximately 4%. Moreover, the crystallization behaviors were analyzed combining with differential scanning calorimetry (DSC), X-ray diffraction (XRD), and scanning electron microscopy (SEM). The mechanical properties and acid and alkali resistance of the prepared glass ceramics were analyzed. This work can not only provide a theoretical reference for controlling crystallization and preparing slag-based glass–ceramic, but also provide experimental technical support for the effective resource utilization of Ti-bearing blast furnace slag.

Experimental procedures

Sample preparation

Ti-bearing blast furnace slag was obtained from an iron and steel plant in China, and the chemical compositions were characterized by X-ray fluorescence spectroscopy (XRF), as showed in Table 1. The CaO/SiO_2 ratio of the original Ti-bearing blast furnace slag was approximately 1.1, and the chemical reagent SiO_2 was added to adjust the R (CaO/SiO_2) of specimens to be 0.3, 0.4, 0.5, and 0.6, respectively. The chemical compositions of the samples are showed in Table 2.

The prepared specimens were ground in an agate mortar for 0.5 h after accurately weighing to mix the various components uniformly. Then, the powder specimens were placed into a corundum crucible, and the temperature was raised from room temperature to 1500 °C in air holding 4 h. After that, the specimens were removed and quenched with water to obtain the basic glass specimens, which were identified by XRD, as showed in Fig. 1.

After grounding the basic glasses into powder with 200 mesh, 1% polyvinyl alcohol and 5% zinc stearate as binders were added. The FYD-30 electric powder compactor was used to press glass powders into the cylinder with a diameter of 8 mm for Vickers hardness detection. The cuboids with 50 × 6 × 6 mm were also pressed for flexural strength detection. The pressed specimens were placed on a platinum sheet and heated to 600 °C for 1 h in a high-temperature tube

Table 1 Chemical composition of Ti-bearing blast furnace slag (wt%)

CaO	SiO_2	Al_2O_3	TiO_2	MgO	Fe_2O_3	Others	CaO/SiO_2
35.00	31.83	13.54	6.71	6.13	1.35	5.44	1.1

Table 2 Chemical composition of basic glass (wt%)

Samples	CaO	SiO_2	Al_2O_3	TiO_2	MgO	Fe_2O_3	Others	CaO/SiO_2
S1	18.95	63.13	7.32	3.63	3.32	0.73	2.94	0.3
S2	22.48	56.21	8.70	4.31	3.94	0.87	3.49	0.4
S3	25.33	50.66	9.80	4.85	4.44	0.98	3.94	0.5
S4	27.67	46.11	10.70	5.30	4.85	1.07	4.30	0.6

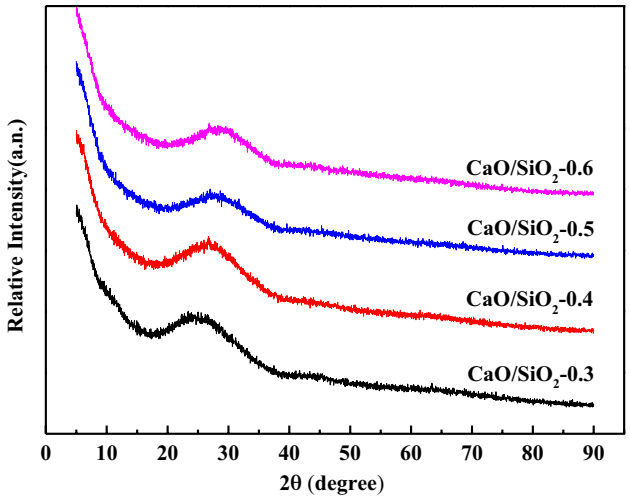

Fig. 1 XRD patterns of basic glasses

furnace to reduce the glass stress and remove the binders. According to the results of DSC, the transition temperature (T_g) of the prepared glasses was determined at the range of 740–760 ℃, and then the nucleation temperature was estimated by 800 ℃, because the optimum nucleation temperature usually lie at 40–80 ℃ above T_g of glasses [35]. Then, the specimens were hold in its crystallization temperature for 1.5 h to obtain the glass ceramics. The specific flowchart is showed in Fig. 2 [36].

Analysis methods

X-ray fluorescence spectroscopy (XRF) (XRF-1800, Shimadzu, Japan) was used to obtain the chemical composition of Ti-bearing blast furnace slag. The basic glass samples were examined by DSC (449F3, NETZSCH, Germany) in air from room temperature to 1300 °C at heating rate of 5 °C/min, to obtain the transition temperature and crystallization temperature. The Fourier transform infrared spectroscopy (FT-IR) (iS50, Thermo Fisher, USA), with a spectral resolution of 4 cm^{-1}, was recorded in the wavenumber range of 400–4000 cm^{-1} to analyze the microstructure of basic glasses. The phase of glass ceramics was identified by X-ray diffraction (XRD) (PANalytical X'Pert Powder, Spectris Pte, Netherlands). The scanning electron microscopy with an energy dispersive spectrometer (SEM–EDS) (JSM-7800F, JEOL, Japan) was used to observe the crystal phase and morphology of glass ceramics.

Regarding the physical performances of the prepared glass ceramics, the density was determined using Eq. (1), as follows:

$$\rho = \frac{m_0}{h * \pi * r^2} \tag{1}$$

where ρ is the density of glass ceramics, m_0 is the mass of glass ceramics, h is the height of cylindrical sample, and r is the radius of cylindrical sample. The vickers hardness was measured by a microhardness-tester (MH-5L, Shanghai,

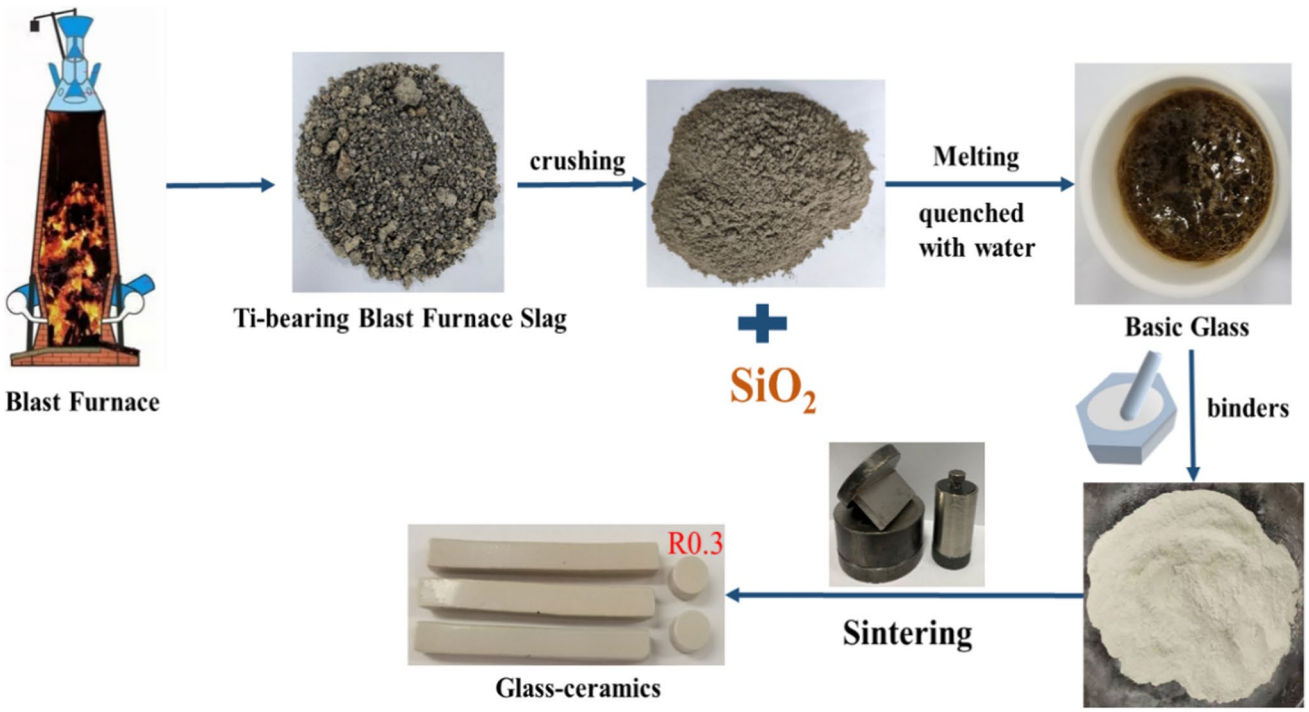

Fig. 2 The specific preparation process of Ti-bearing blast furnace slag-based glass ceramics [36]

China) with a measuring force of 300 N and a load time of 15 s. Besides, the electronic universal material testing machine (CMT4303, MTS, American) was used to detect the flexural strength of specimens with a span of 40 mm and the descent speed of 0.5 mm/min, and the flexural strength values were calculated by the equation according to GB/T 6569–2006, as shown as Eq. (2):

$$\sigma_f = \frac{3FL}{2bd^2} \tag{2}$$

where σ_f is the flexural strength (MPa), F is the maximum load (N), and L is the lower span of fixture(mm). Besides, b and d are the width and height of the sample (mm), respectively. Moreover, the surface and weight changes were observed after immersing the glass ceramics in 5% H_2SO_4 and 5% NaOH solutions for 24 h to evaluate the acid and alkali corrosion resistance of glass ceramics. The chemical stability was calculated by weighing the samples before corrosion (m_0) and after corrosion (m_1):

$$\mathrm{K}(\%) = \frac{m_1}{m_0} \times 100 \tag{3}$$

Results and discussion

Crystallization behaviors of Ti-bearing blast furnace slag-based glass ceramics

The DSC curves of Ti-bearing blast furnace slag-based glass samples with different CaO/SiO_2 ratio at heating rate of 5℃/min are showed in Fig. 3(a). The transition temperature (T_g) and crystallization temperature (T_p) can be determined as the endothermic and exothermic peak temperature, respectively. The variations in transition and crystallization temperature of the prepared basic glass samples are showed in Fig. 3(b), demonstrating that the crystallization temperature obviously decreased with the increasing CaO/SiO_2 ratio, and only negligible changes of T_g were detected. Besides, as the increase of CaO/SiO_2 ratio, the crystallization peak intensity increased, indicating that the crystallization ability enhanced. Because Ca^{2+} ions has an effect on enriching oxygen, it accelerated to destroy the bridging oxygen bond of Si–O-Si units in the Si–O tetrahedron [32, 37], thereby creating more non-bridging oxygen bonds, reducing the degree of network polymerization, and decreased the crystallization activation energy, that resulted in stronger crystallization. This can be further confirmed from the FT-IR spectra of basic glasses, as showed in Fig. 4. According to previous studies [38–40], the FT-IR spectra curves can be divided into two domains: the 600–800, and 800–1200 cm^{-1} bands. The weaker band at 600–800 cm^{-1} was attributed

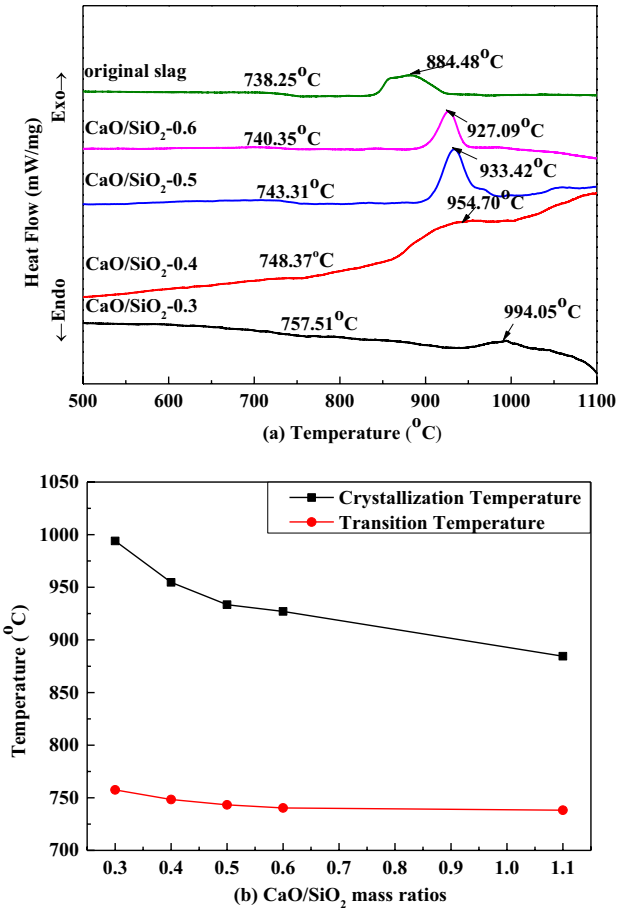

Fig. 3 The result of DSC with different CaO/SiO_2 mass ratios. (**a**) DSC curve of basic glass; (**b**) the changes of transition and crystallization temperature

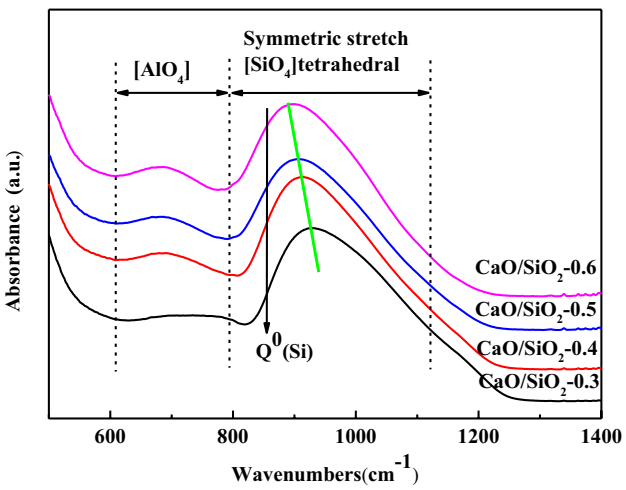

Fig. 4 FTIR spectra of prepared glasses with different CaO/SiO_2 ratios between 500 and 1400 cm^{-1}

to the bending vibrations of [AlO_4]. The highest intensity bands in 800–1200 cm^{-1} range corresponded to the stretching vibrations of [SiO_4] tetrahedral network, and the main peak shifted to low wave number with CaO/SiO_2 ratios increasing. Moreover, it was observed that the intensity of the band centered at about 845 cm^{-1} gradually strengthen with the increase of CaO/SiO_2 ratio, which was assigned to Q^0 (Q is the tetrahedron with Si atom as the center and n is the amount of bridging oxygen in it) [38]. The specific schematic diagram of [SiO_4] tetrahedral, [AlO_4] tetrahedral, and Si–O-Si bridging oxygen is showed in Fig. 5. Si–O-Si means that the two [SiO_4] structure units are connected by sharing one oxygen, which is here called a bridging oxygen. The oxygen with only one [SiO_4] connected is called non-bridging oxygen. When four oxygens in one [SiO_4] unit are non-bridging oxygen, this is called Q^0 which is isolated island structure. The increase of Q^0 indicated the decrease of polymerization degree. Therefore, the degree of polymerization of the investigated glasses decreased with increase of CaO/SiO_2 ratio, so the atoms' transfer for crystallization became easier, which resulted in a decreased crystallization temperature and an increased crystallization ability.

The crystal phases of Ti-bearing blast furnace slag-based glass ceramics were analyzed by combination with XRD and SEM–EDS. XRD patterns of the glass–ceramic samples with different CaO/SiO_2 ratios are showed in Fig. 6. It can be observed that the main crystal phases transformed from

Fig. 5 Schematic diagram of [SiO_4] tetrahedral, [AlO_4] tetrahedral, and Si–O-Si bridging oxygen

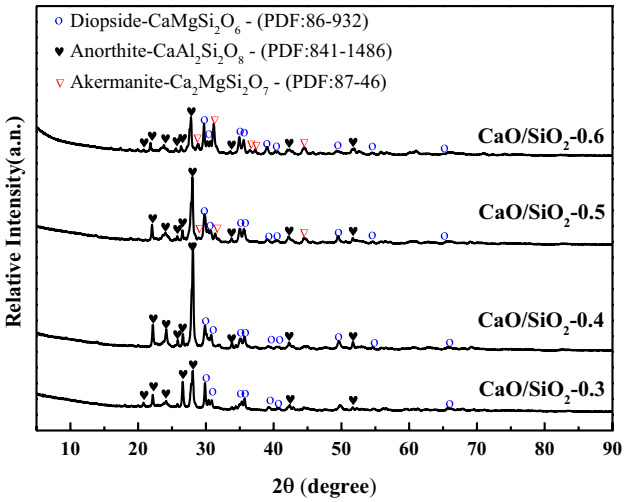

Fig. 6 XRD patterns of glass ceramics with different CaO/SiO_2 mass ratios

$CaAl_2Si_2O_8$ and $CaMgSi_2O_6$ to $CaAl_2Si_2O_8$, $CaMgSi_2O_6$, and $Ca_2MgSi_2O_7$ as the CaO/SiO_2 ratio increased from 0.3 to 0.6. When CaO/SiO_2 ratio was less than 0.5, the ratio of Ca and Si in the precipitated crystals was 1/2. Due to the increase of CaO/SiO_2 ratio, the crystal phase of $Ca_2MgSi_2O_7$ containing larger ratio of Ca and Si was precipitated at $CaO/SiO_2 = 0.5$, and it increased as CaO/SiO_2 ratio continued to increase. As seen from the XRD patterns, the crystals were still dominated by $CaAl_2Si_2O_8$ as an increased CaO/SiO_2 ratio.

Moreover, to further explore the shape and distribution of crystals, the glass ceramics were polished and analyzed by SEM–EDS, which are exhibited in Fig. 7. It can be observed that when CaO/SiO_2 ratio was 0.3, the massive crystals and fine needle-like crystals were observed in the SEM images, the needle-like crystals grown around the glass phase, and there were still a lot of glass phases, and the crystals distribution in the glass was not uniform. With the increase of CaO/SiO_2 ratio, the glass phase decreased, the crystal phase and the glass phase were uniformly distributed, and the crystal shape changed to dendritic, the size decreased. When CaO/SiO_2 ratio reached 0.6, the size of dendritic crystals in glass ceramics increased. Combining the DSC curve and FT-IR analysis results showed that when CaO/SiO_2 ratio increased, the glass was easier to crystallize. Glasses have proper crystallization ability that can make the crystal size small and uniformly distributed in the glass ceramics, but when the crystallization ability is too strong, the crystals will grow excessively, which will increase the crystal size. In addition, it can be observed that the results of EDS point detections showed that the crystal phase in the glass ceramics was approximately to $CaAl_2Si_2O_8$. Other phases were not identified which may be due to their low content and/

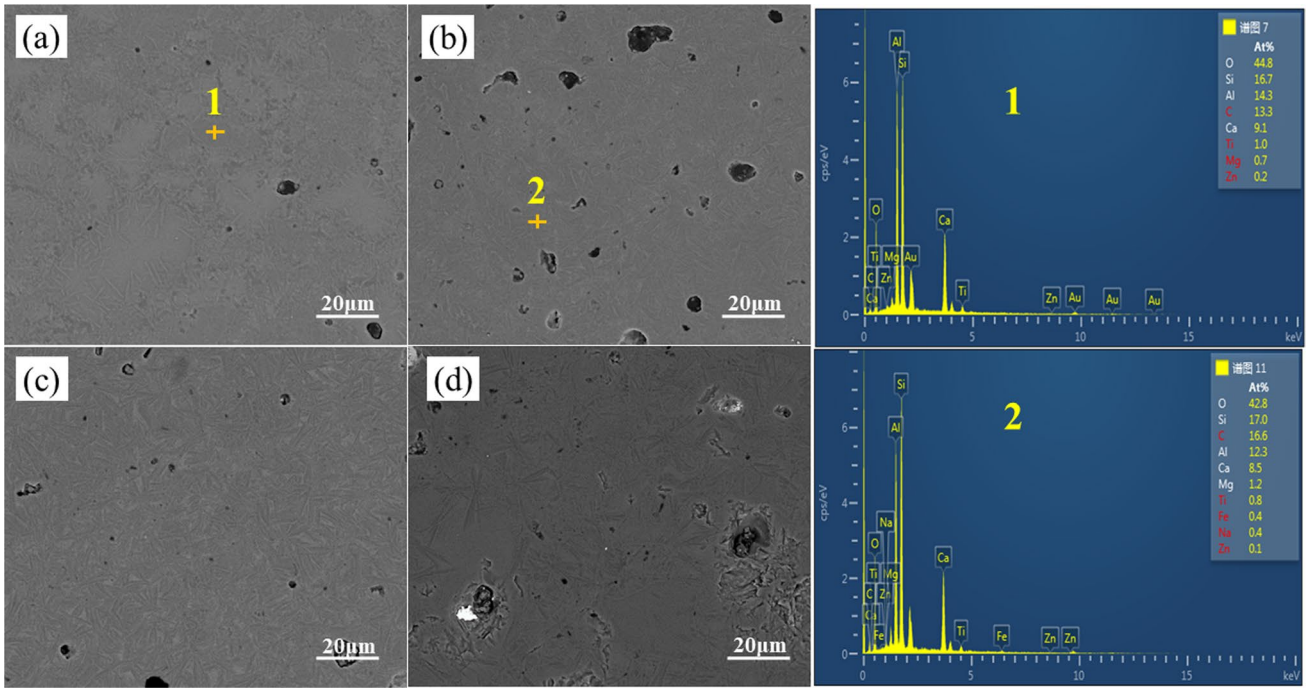

Fig. 7 SEM images of the polished slag-based glass ceramics. (**a**) S1, (**b**) S2, (**c**) S3, and (**d**) S4

or small size. The primary crystal phase is consistent with the XRD results.

The crystallite phase in glass ceramics is as the framework, and the glass phase is as a continuous phase to bond the crystallite phases together. For the case of fine crystal grains, dense, and uniform distribution, it can further improve the overall performance of the material. Therefore, it can be regarded as a good crystal distribution state when the CaO/SiO_2 ratio is 0.5.

Properties of Ti-bearing blast furnace slag-based glass ceramics

Density and vickers hardness analysis

The physical properties of the prepared glass ceramics are presented in Table 3, including density, vickers hardness, and flexural strength. The density of all specimens were in the range of 2.68–2.85 g/cm^3. Compared with the original Ti-bearing blast furnace slag-based glass–ceramic (the density is 2.16 g/cm^3), the density increased significantly with a decreased CaO/SiO_2 ratio. As showed in Table 3, as increasing CaO/SiO_2 ratio, the vickers hardness gradually decreased, since the glass ceramics with the CaO/SiO_2 ratio of 0.3 had relatively few crystals, which showed the highest vickers hardness of 1045.10 MPa. According to the results of DSC, the crystallization ability increased with the increase of CaO/SiO_2 ratio, but excessive crystallization ability may reduce the hardness of glass ceramics[25], and the grain growth may be another reason. According to the Hall–Petch formula, the relationship between hardness of a bulk material and grain size can be described by Eq. (4) [30, 41, 42]:

$$H_g = H_0 + k/\sqrt{D} \tag{4}$$

where H_g is the hardness of grain interior;D is the grain size; H_0 is the intrinsic hardness of the grain and k is a constant. Equation (4) indicates that the increase of grain size will worsen the hardness of sample. Thus, with increasing CaO/SiO_2 ratio, the crystallization ability increased and

Table 3 The physical properties of Ti-bearing blast furnace slag-based glass ceramics

Samples	S1	S2	S3	S4	Original slag
Density (g cm^{-3})	2.68 ± 0.05	2.71 ± 0.05	2.79 ± 0.05	2.85 ± 0.05	2.16 ± 0.05
Vickers hardness (MPa)	1045.10 ± 52.75	959.24 ± 23.06	882.66 ± 25.41	789.63 ± 40.45	—
Flexural strength (MPa)	72.60 ± 10.87	85.56 ± 7.74	109.58 ± 7.51	61.81 ± 9.84	26.09 ± 0.54

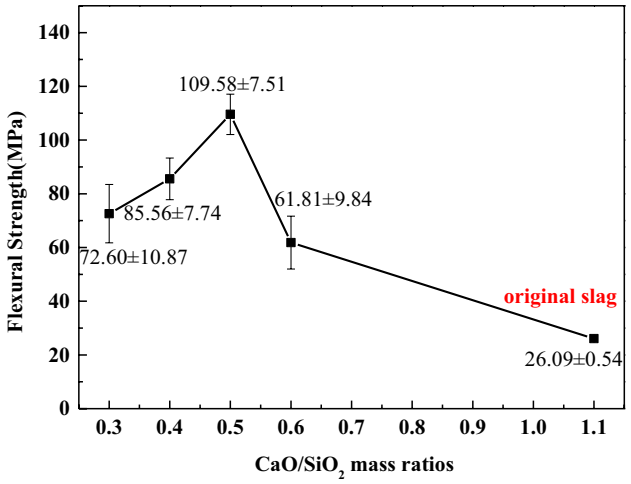

Fig. 8 The change of the flexural strength of glass–ceramic with different CaO/SiO_2 mass ratios

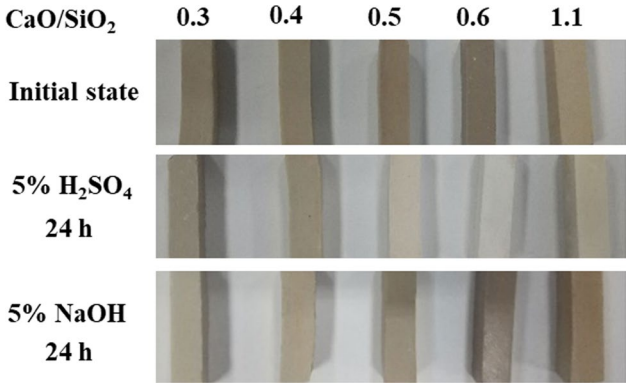

Fig. 9 The surface condition of the glass ceramics before and after the acid and alkali resistance test

the crystal gradually grown up, so the vickers hardness decreased.

Flexural strength performance analysis

The effect of CaO/SiO_2 ratio on flexural strength of the glass ceramics is showed in Fig. 8. The flexural strength first increased and then decreased as the CaO/SiO_2 ratio increased from 0.3 to 1.1, and the maximum flexural strength value of 109.58 MPa was obtained at $CaO/SiO_2 = 0.5$. Besides, compared with the glass–ceramic prepared by the original Ti-bearing blast furnace slag, decreasing the CaO/SiO_2 ratio significantly improved the flexural strength of the glass–ceramic. According to the results of SEM and DSC, the crystallization ability increased with the increase of CaO/SiO_2 ratio, and when the CaO/SiO_2 ratio was 0.5, the largest number of small-sized crystals was formed in glass ceramics and was uniformly distributed, so the glass ceramics at this condition had excellent flexural performance. As the CaO/SiO_2 ratio continued to increase, the size of crystals in the glass ceramics increased and the flexural strength decreased. It can be showed that within a certain range of crystallization ability, the increase of crystallization ability was helpful for improving the flexural strength, while too high crystallization ability was not conducive. This is consistent with the results of Hou et al. [30].

Acid and alkali resistance performance analysis

The prepared glass ceramics were immersed in 5% H_2SO_4 and 5% NaOH solutions for 24 h. Figure 9 shows the change of the sample surface before and after acid and alkali corrosion test. It can be observed that the glass ceramics showed a certain amount of fading after soaking in 5% H_2SO_4 solution for 24 h, especially at high alkalinity, indicating that the acid resistance performance was slightly weakened as an increased CaO/SiO_2 ratio. However, no obvious changes were observed on the surface of samples after soaking in 5% NaOH solution for 24 h. The weight changes of the glass–ceramic samples were calculated to evaluate the acid and alkali resistance performance, listed in Table 4. Compared with the glass ceramics prepared from the original slag, reducing the ratio of CaO/SiO_2 had a certain positive effect on the acid and alkali resistance of glass ceramics. Therefore, it can be concluded that all of the prepared glass ceramics showed good acid and alkali resistance, especially the alkali resistance, all over 99.9%.

The results of flexural strength, hardness, and corrosion have been compared to other glass ceramics prepared by blast furnace slag [43–46]. The prepared glass ceramics showed excellent properties, such as flexural strength, acid resistance, and alkali resistance for the samples S2 and S3 (Table 5). The flexural strength of the studied titanium-containing blast furnace slag glass ceramics can reach up to 109.58 MPa at $CaO/SiO_2 = 0.5$. The decrease of CaO/SiO_2 from 1.1 to 0.5, and the flexural strength significantly increased from 26.09 to 109.58 MPa. On the whole, the flexural strength of the prepared glass ceramics is slightly higher than that of most other blast furnace slags. Although the flexural strength was slightly lower than that of the glass ceramics prepared by Deng et al. [45], the current glass ceramics exhibited better resistance to acid and alkali corrosion.

Conclusions

In this work, a series glass ceramics were successfully prepared from Ti-bearing blast furnace slag. The effect of CaO/SiO_2 ratio on the crystallization behaviors, mechanical properties, and acid and alkali resistance properties of the prepared

Table 4 The acid and alkali resistance performance of the glass ceramics with different ratios of CaO/SiO_2

Samples	S1	S2	S3	S4	Original slag
Acid resistance(%)	99.89 ± 0.10	99.78 ± 0.10	98.44 ± 0.10	98.21 ± 0.10	96.40 ± 0.10
Alkali resistance(%)	99.94 ± 0.10	99.93 ± 0.10	99.94 ± 0.10	99.94 ± 0.10	99.88 ± 0.10

Table 5 Comparison of main properties of glass ceramics prepared with better properties with those of others' works

Samples	Flexural strength (MPa)	Hardness (MPa)	Acid resistance (%)	Alkali resistance (%)
S2	85.56 ± 7.74	959.24 ± 23.06	99.78 ± 0.10	99.93 ± 0.10
S3	109.58 ± 7.51	882.66 ± 25.41	98.44 ± 0.10	99.94 ± 0.10
Blast furnace slag-based [43]	102.20	-	99.72	99.67
Blast furnace slag-based [44]	-	612.00 ± 36.00	99.72	95.50
Blast furnace slag-based [45]	196.69 ± 9.14	-	97.05 ± 0.04	98.04 ± 0.04
Blast furnace slag-based [46]	96.00	-	99.98	99.77

Ti-bearing blast furnace slag-based glass ceramics were investigated. The following conclusions can be drawn:

(1) The crystallization temperature obviously decreased with the increase of CaO/SiO_2 ratio, and the higher CaO/SiO_2 ratios leaded to stronger crystallization ability.
(2) The main crystal phases transformed from $CaAl_2Si_2O_8$ and $CaMgSi_2O_6$ to $CaAl2Si_2O_8$, $CaMgSi_2O_6$, and $Ca_2MgSi_2O_7$ as the CaO/SiO_2 ratio increased from 0.3 to 0.6. When the CaO/SiO_2 increased to 0.5, a small amount of akermanite precipitated.
(3) The vickers hardness gradually decreased, and the flexural strength first increased and then decreased with an increased CaO/SiO_2. The glass ceramic with $CaO/SiO_2 = 0.5$ exhibited the highest flexural strength of 109.58 MPa. The prepared glass ceramics showed good acid and alkali resistance (> 98.30%), especially alkali resistance. Therefore, the best candidate for CaO/SiO_2 ratio in the investigated Ti-bearing blast furnace slag-based glass ceramics was selected as 0.5.

Funding This work was supported by Fundamental and Frontier Research Project of Chongqing (cstc2018jcyjAX0791).

Declarations

Conflict of interest The authors declare no competing interests.

References

1. Liu, H., Lu, H., Chen, D., Wang, H., Xu, H., Zhang, R.: Preparation and properties of glass–ceramics derived from blast-furnace slag by a ceramic-sintering process. Ceram. Int. **35**, 3181–3184 (2009)
2. Zhang, S.G., Yang, J., Liu, B., Pan, D.A., Wu, C.I., Volinsky, A.A.: One-step crystallization kinetic parameters of the glass-ceramics prepared from stainless steel slag and pickling sludge. J. Iron Steel Res. Int. **23**, 220–224 (2016)
3. Teixeira, S.R., Souza, A.E., Carvalho, C.L., Reynoso, V.C., Romero, M., Rincón, J.M.: Characterization of a wollastonite glass-ceramic material prepared using sugar cane bagasse ash (SCBA) as one of the raw materials. Mater. Charact. **98**, 209–214 (2014)
4. Pei, F.J., Zhu, G.H., Li, P., Guo, H.W., Yang, P.: Effect of Fe_2O_3 and MgO on the crystallization behaviour, sinterability and properties of the $CaO\text{-}Al_2O_3\text{-}SiO_2$ glass-ceramics. J. Aust. Ceram. Soc. **56**, 979–986 (2020)
5. Li, B., Xia, Q., Wang, Z.Y.: Effect of MnO on the crystallization, microstructure, and properties of $MgO\text{-}Al_2O_3\text{-}SiO_2$ glass-ceramics. J. Aust. Ceram. Soc. **57**, 927–932 (2021)
6. Rawlings, R., Wu, J., Boccaccini, A.: Glass-ceramics: their production from wastes—a review. J. Mater. Sci. **41**, 733–761 (2006)
7. Zhao, Y., Chen, D., Bi, Y., Long, M.: Preparation of low cost glass–ceramics from molten blast furnace slag. Ceram. Int. **38**, 2495–2500 (2012)
8. Ren, S., Aldahri, T., Liu, W., Liang, B.: CO_2 mineral sequestration by using blast furnace slag: from batch to continuous experiments. Energy. **214**, 118975 (2021)
9. Kozlowski, M., Khater, G., Olesik, P., Mahmoud, M.: Preparation and characterization of lightweight glass-ceramics based on industrial wastes. J. Aust. Ceram. Soc. **56**, 11–20 (2020)
10. Zhang, W., He, F., Xiao, Y., Xie, M., Li, F., Xie, J., Yang, H., Li, Z.: Structure, viscosity, and crystallization of glass melt from molten blast furnace slag. Int. J. Appl. Glass Sci. **11**, 676–684 (2020)

11. Francis, A.: Non-isothermal crystallization kinetics of a blast furnace slag glass. J. Am. Ceram. Soc. **88**, 1859–1863 (2005)
12. Liu, W., Aldahri, T., Xu, C., Li, C., Rohani, S.: Synthesis of sole gismondine-type zeolite from blast furnace slag during CO_2 mineralization process. J. Environ. Chem. Eng. **9**, 104652 (2020)
13. Yang, J., Zhang, S.-G., Liu, B., Pan, D.-A., Wu, C.-L., Volinsky, A.A.: Effect of TiO_2 on crystallization, microstructure and mechanical properties of glass-ceramics. J. Iron Steel Res. Int. **22**, 1113–1117 (2015)
14. Hu, A., Li, M., Mao, D.: Controlled crystallization of glass–ceramics with two nucleating agents. Mater. Charact. **60**, 1529–1533 (2009)
15. Montoya-Quesada, E., Villaquiran-Caiced, M.A., de Gutierrez, R.M., Munoz-Saldana, J.: Effect of ZnO content on the physical, mechanical and chemical properties of glass-ceramics in the CaO-SiO_2-Al_2O_3 system. Ceram. Int. **46**, 4322–4328 (2020)
16. Francis, A.: Conversion of blast furnace slag into new glass-ceramic material. J. Eur. Ceram. Soc. **24**, 2819–2824 (2004)
17. Hou, Y., Zhang, G.H., Chou, K.C.: Effect of atmosphere control on magnetic properties of CaO-Al_2O_3-SiO_2-Fe_3O_4 glass ceramics. J. Eur. Ceram. Soc. **41**, 2663–2673 (2020)
18. Fang, J., Sun, L., Guo, S., Liu, C., Zhang, J.: Study of Li_2O addition on crystallization behavior and thermal expansion properties of CaO-Al_2O_3–SiO_2 (CAS) glass-ceramic and its application for joining SiC ceramic. J. Eur. Ceram. Soc. **41**, 1817–1827 (2021)
19. Araujo, M.C., Botta, W.J., Kaufmann, M.J., Angelica, R.S., Mercury, J.M., Cabral, A.A.: Residual glass and crystalline phases in a barium disilicate glass–ceramic. Mater. Charact. **110**, 192–196 (2015)
20. Rajavaram, R., Kim, H., Park, J., Lee, C.H., Cho, W.S., Lee, J.: Bridging between the physical properties: structure and density of CaO-SiO2-Al2O3 melts at CaO/SiO2=1.3 and different mole% of Al2O3. Ceram. Int. **45**, 19409–19414 (2019)
21. Xue, J.W., Zhong, J.W., Mao, Y.R., Xu, C.H., Liu, W., Huang, Y.Q.: Effect of CuO on crystallisation and properties of red R_2O-CaO-MgO-Al_2O_3-SiO_2 glass-ceramics from granite wastes. Ceram. Int. **46**, 23186–23193 (2020)
22. Li, Z., Wu, J., Song, L., Huang, Y.: Effect of composition on sinter-crystallization and properties of low temperature co-fired α-cordierite glass–ceramics. J. Eur. Ceram. Soc. **34**, 3981–3991 (2014)
23. Valderrama, D.M.A., Cuaspud, J.A.G., Roether, J.A., Boccaccini, A.R.: Development and characterization of glass-ceramics from combinations of slag, fly ash, and glass cullet without adding nucleating agents. Materials. **12**, 2032 (2019)
24. Chang, Z.Y., Jiao, K.X., Ning, X.J., Zhang, J.L.: Novel approach to studying influences of Na_2O and K_2O additions on viscosity and thermodynamic properties of BF slags. Metall. Mater. Trans. B. **50**, 1399–1406 (2019)
25. Tang, X.L., Zhang, Z.T., Guo, M., Zhang, M., Wang, X.D.: Viscosities behavior of CaO-SiO_2-MgO-Al_2O_3 slag with low mass ratio of CaO to SiO_2 and wide range of Al_2O_3 content. J Iron Steel Re Int **18**, 1–6 (2011)
26. Tabit, K., Hajjou, H., Waqif, M., Saadi, L.: Effect of CaO/SiO_2 ratio on phase transformation and properties of anorthite-based ceramics from coal fly ash and steel slag. Ceram. Int. **46**, 7550–7558 (2020)
27. Yang, Z., Lin, Q., Lu, S., He, Y., Liao, G., Ke, Y.: Effect of CaO/SiO_2 ratio on the preparation and crystallization of glass-ceramics from copper slag. Ceram. Int. **40**, 7297–7305 (2014)
28. Li, B., Li, W., Zheng, J.: Effect of SiO_2 content on the sintering kinetics, microstructures and properties of BaO-Al_2O_3-B_2O_3-SiO_2 glass-ceramics for LTCC application. J. Alloys Compd. **725**, 1091–1097 (2017)
29. Zhou, X., Bo, L., Zhang, S., Ning, H.: Effect of Ca/Si ratio on the microstructures and properties of CaO-B_2O_3-SiO_2 glass-ceramics. J. Mater. Sci. Mater. Electron. **20**, 262–266 (2009)
30. Hou, Y., Zhang, G.-H., Chou, K.C., Fan, D.: Effects of CaO/SiO_2 ratio and heat treatment parameters on the crystallization behavior, microstructure and properties of SiO_2-CaO-Al_2O_3-Na_2O glass ceramics. J. Non-Cryst. Solids. **538**, 120023 (2020)
31. Fu, Y., Li, P., Tao, H., Zhang, L., Xin, M., Chang, Y., Xia, Y., Zhou, H.: The effects of Ca/Si ratio and B_2O_3 content on the dielectric properties of the CaO–B_2O_3 –SiO_2 glass–ceramics. J. Mater. Sci. Mater. Electron. **30**, 14053–14060 (2019)
32. Jia, R., Deng, L., Yun, F., Li, H., Zhang, X., Jia, X.: Effects of SiO_2/CaO ratio on viscosity, structure, and mechanical properties of blast furnace slag glass ceramics. Mater. Chem. and Phys. **233**, 155–162 (2019)
33. Xie, C., Gui, Y., Song, C., Hu, B.: Effect of CaO/SiO_2 and heat treatment on the microstructure of glass-ceramics from blast furnace slag. Ceram. Silik. **60**, 146–151 (2016)
34. Lai, F., Leng, M., Li, J., Liu, Q.: The crystallization behaviors of SiO_2-Al_2O_3-CaO-MgO-TiO_2 glass-ceramic systems. Curr. Comput.-Aided Drug Des. **10**, 794 (2020)
35. Wang, Y.C., Liu, P.J., Luo, G.P., Liu, Z., Cao, P.F.: Optimization of heat treatment of glass-ceramics made from blast furnace slag. High Temp. Mater. Proc. **39**, 539–544 (2020)
36. Jiao, M.J., Wu, H.M., Li, Z.Y., Lai, F.F., Li, J.L.: Effect of Cr_2O_3 on the crystallization, structure and properties of Ti-bearing blast furnace slag-based glass ceramics. J. Asian Ceram, Soc (2021).. (**In press**)
37. Tarragó, M., Esteves, H., Garcia-Valles, M., Martínez, S., Neuville, D.: Effect of Ca in P-doped basaltic glass-ceramics: application to waste inertization. Mater. Lett. **220**, 266–268 (2018)
38. Li, J., Sun, Y., Li, Z., Zhang, Z.: Short-range and medium-range structural order in CaO–SiO_2–TiO_2–B_2O_3 glasses. ISIJ Int. **56**, 752–758 (2016)
39. Zhu, X., Mai, C., Li, M.: Effects of B_2O_3 content variation on the Bi ions in Bi_2O_3–B_2O_3–SiO_2 glass structure. J. Non-Cryst. Solids. **388**, 55–61 (2014)
40. Lai, F., Yao, W., Li, J.: Effect of B_2O_3 on structure of CaO–Al_2O_3–SiO_2–TiO_2–B_2O_3 glassy systems. ISIJ Int. **60**, 1596–1601 (2020)
41. Wang, J., Shaw, L.L.: Grain-size dependence of the hardness of submicrometer and nanometer hydroxyapatite. J. Am. Ceram. Soc. **93**, 601–604 (2010)
42. Gaida, N.A., Nishiyama, N., Masuno, A., Holzheid, A., Ohfuji, H., Schürmann, U., Szillus, C., Kulik, E., Bednarcik, J., Beermann, O.: Synthesis of Al_2O_3/SiO_2 nano-nano composite ceramics under high pressure and its inverse Hall-Petch behavior. J. Am. Ceram. Soc. **100**, 323–332 (2017)
43. Wang, Y.C., Liu, P.J., Luo, G.P., Liu, Z., Cao, P.F.: Optimization of heat treatment of glass-ceramics made from blast furnace slag. High Temp. Mat. Pr-Isr. **39**, 539–544 (2020)
44. Montoya-Quesada, E., Villaquirán-Caicedo, M. A., Gutiérrez, Ruby Mejía de.: New glass-ceramic from ternary–quaternary mixtures based on Colombian industrial wastes: Blast furnace slag, cupper slag, fly ash and glass cullet. Boletín de la Sociedad Española de Cerámica y Vidrio. (2021) (**In press**)
45. Deng, L., Jia, R., Yun, Fei, Zhang, X., Li, H., Zhang, M., Jia, X., Ren, D., Li, B.: Influence of Cr_2O_3 on the viscosity and crystallization behavior of glass ceramics based on blast furnace slag. Mater. Chem. Phys. **240**, 122212 (2020)
46. Zhao, W., Huang, X., Yan, B., Hu, S., Guo, H., Chen, D.: Recycling of blast furnace slag and fluorite tailings into diopside-based glass-ceramics with various nucleating agents' addition. Sustainability. **13**, 11144 (2021)